Energy transfer and frequency upconversion in Yb³⁺–Er³⁺-doped PbO-GeO₂ glass containing silver nanoparticles

L.R.P. Kassab · F.A. Bomfim · J.R. Martinelli · N.U. Wetter · J.J. Neto · Cid B. de Araújo

Abstract We report the infrared-to-visible frequency upconversion in Er³⁺–Yb³⁺-codoped PbO-GeO₂ glass containing silver nanoparticles (NPs). The optical excitation is made with a laser at 980 nm in resonance with the $^2F_{5/2} \rightarrow {}^2F_{7/2}$ transition of Yb³⁺ ions. Intense emission bands centered at 525, 550, and 662 nm were observed corresponding to Er³⁺ transitions. The simultaneous influence of the Yb³⁺ → Er³⁺ energy transfer and the contribution of the intensified local field effect due to the silver NPs give origin to the enhancement of the whole frequency upconversion spectra.

PACS 42.70.Ce · 78.55.-m · 78.55.Qr · 78.90.+t · 81.05.Pj

Phenomena related to the interaction of light with rare-earth-doped (RE-doped) glasses containing metallic nanoparticles (NPs) have been attracting large attention due to their relevance for a variety of applications such as colored displays, optical amplifiers as well as optical sensors. In particular,

L.R.P. Kassab
Laboratório de Vidros e Datações da FATEC-SP,
CEETEPS/UNESP, 01124-060 São Paulo, SP, Brazil

F.A. Bomfim · J.R. Martinelli
Centro de Ciências e Tecnologia de Materiais—IPEN,
05508-900 São Paulo, SP, Brazil

N.U. Wetter · J.J. Neto
Centro de Lasers e Aplicações—IPEN, 05508-900 São Paulo, SP, Brazil

C.B. de Araújo (✉)
Departamento de Física, Universidade Federal de Pernambuco, 50670-901 Recife, PE, Brazil
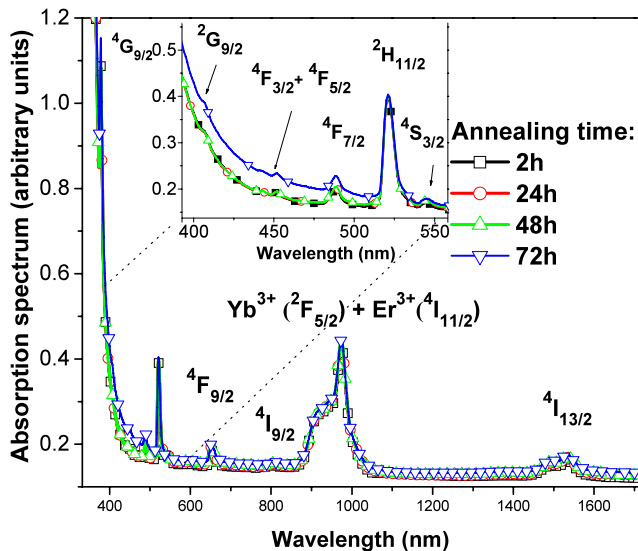e-mail: cid@df.ufpe.br

the surface-plasmon-enhanced (SP-enhanced) luminescence observed in RE-doped glasses containing metallic NPs has been studied by many authors [1–11].

Among the systems of interest the heavy metal oxide (HMO) glasses are known as excellent materials for photonic applications because of their specific characteristics such as: large mechanical resistance, high chemical durability and thermal stability, large transmission window (from 400 to 4500 nm), high refractive index, large nonlinear optical response, and low cutoff phonon energy (400–800 cm⁻¹) [1].

In the past years the synthesis and the characterization of HMO glasses doped with RE ions and containing metallic NPs were reported [7–11]. For instance, down-conversion luminescence enhancement was reported for Pr³⁺-doped lead-germanate oxide (PGO) glass containing silver NPs [7]. The increase of Eu³⁺ luminescence due to the presence of gold NPs in tellurite glasses was observed and characterized [8]. Studies of SP-enhanced frequency upconversion (UC) in Pr³⁺-doped tellurium-oxide glasses with silver NPs were reported in [9].

Also, recently we have demonstrated enhancement of ~100% in the infrared-to-green UC process in Er³⁺-doped PGO glass containing silver NPs [10]. The excitation was made at 980 nm and the growth of the UC intensity at 530 and 550 nm was attributed to the increased local field in the proximity of the NPs. Unfortunately, even in the presence of the NPs the UC luminescence of the Er³⁺-doped PGO is limited by the relatively small absorption cross-section of Er³⁺ ions at 980 nm. The red luminescence at 662 nm having wavelength far from the SP resonance wavelength, λ_{SP}, is less influenced by the presence of spherical silver NPs. However, it may be intensified if particles with different shapes and aggregates of NPs are present. On the other hand, PGO glass doped with Er³⁺ and Yb³⁺, without silver

Fig. 1 Absorption spectra of Er^{3+}–Yb^{3+}-codoped PbO-GeO$_2$ glasses containing silver NPs for different heat-treatment durations

NPs, present increased red luminescence due to the energy transfer (ET) from Yb^{3+} to Er^{3+} ions [12, 13].

In this letter we demonstrate improvement of the UC luminescence efficiency of Er^{3+} ions in PGO glass containing silver NPs by codoping the samples with Yb^{3+} ions. We show that the combined effect of the silver NPs and the efficient ET from resonantly excited Yb^{3+} ions contribute to the enhancement of the whole UC spectrum. The large absorption cross-section of the Yb^{3+} ions at 980 nm allows the increase of the red luminescence in such a way that it may reach intensities comparable with the green emissions.

The PGO glass composition studied was 41 PbO-59 GeO$_2$ (in mol%). For the experiments we added 0.5 wt% of Er_2O_3, 3.0 wt% of Yb_2O_3, and 1.0 wt% of AgNO$_3$ to the original composition. The samples were obtained by melting the starting oxide powders in an alumina crucible for 1 h at 1200°C, quenching and annealing in air in a preheated brass mold, and annealing at 420°C for 2 h. After the cooling the samples were polished and then annealed for different durations ($\tau_A = 24$, 48, and 72 h) to reduce the Ag^+ ions to Ag^0, in order to nucleate silver NPs.

Transmission electron microscopy (TEM) using a 200 kV equipment was performed to investigate the nucleation and growth of the NPs.

The linear optical absorption spectra were measured at room temperature in the 300–1700 nm range and the frequency UC spectra (infrared-to-visible conversion) were excited with a CW diode laser (7 W, 980 nm). The luminescence signal was dispersed by a monochromator fitted with a photomultiplier.

Figure 1 presents the absorption spectra of the Er^{3+}–Yb^{3+}-codoped PGO glass containing silver NPs in the visible and in the near-infrared regions. Absorption bands at-
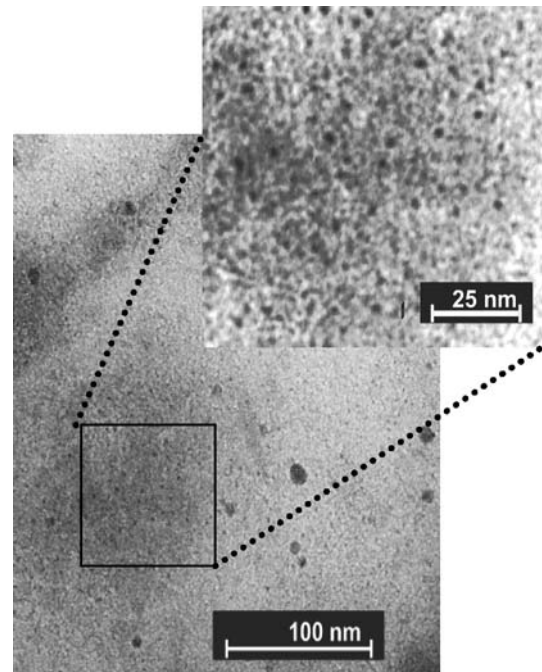

Fig. 2 TEM images of the samples annealed for 48 h at 420°C

tributed to the $4f$–$4f$ transitions of Er^{3+} ions corresponding to the transitions starting from the ground state ($^4I_{15/2}$) to the excited states are observed. The intense absorption band at ≈ 980 nm is mainly due to the $^2F_{7/2} \rightarrow {}^2F_{5/2}$ transition of Yb^{3+} ions that overlaps with the weaker $^4I_{15/2} \rightarrow {}^4I_{11/2}$ transition of the Er^{3+} ions. The absorption band related to the SP is not observed because the amount of the NPs is not enough to originate a strong band. With the basis on the dielectric function of silver [14] and the refractive index of PGO glass (≈ 2), we estimated λ_{SP} to be located in the range of ~ 420 to ~ 500 nm. However, the presence of the silver NPs in the PGO samples is confirmed by electron microscopy.

Figure 2 shows a TEM image corresponding to the sample annealed for 48 h at 420°C. The metallic NPs have average diameter of 2.5 nm but we also observed the presence of larger particles and aggregates. The samples heat-treated for shorter time intervals present NPs with smaller average diameter.

Figure 3a shows the emission spectra of the Er^{3+}–Yb^{3+}-codoped PGO samples for different anneal durations, τ_A. Emission bands centered at 525, 550, and 662 nm that correspond to the transitions $^2H_{11/2} \rightarrow {}^4I_{15/2}$, $^4S_{3/2} \rightarrow {}^4I_{15/2}$, and $^4F_{9/2} \rightarrow {}^4I_{15/2}$, respectively, are observed. Figure 3b shows that the relative intensity of the UC bands can be adjusted by an appropriate choice of τ_A that controls the amount of silver NPs formed in the sample.

Figure 4 presents a simplified energy level diagram for the Er^{3+} and the Yb^{3+} ions. Because the laser wavelength is in resonance with the transition $^2F_{5/2} \rightarrow {}^2F_{7/2}$ (Yb^{3+}) and
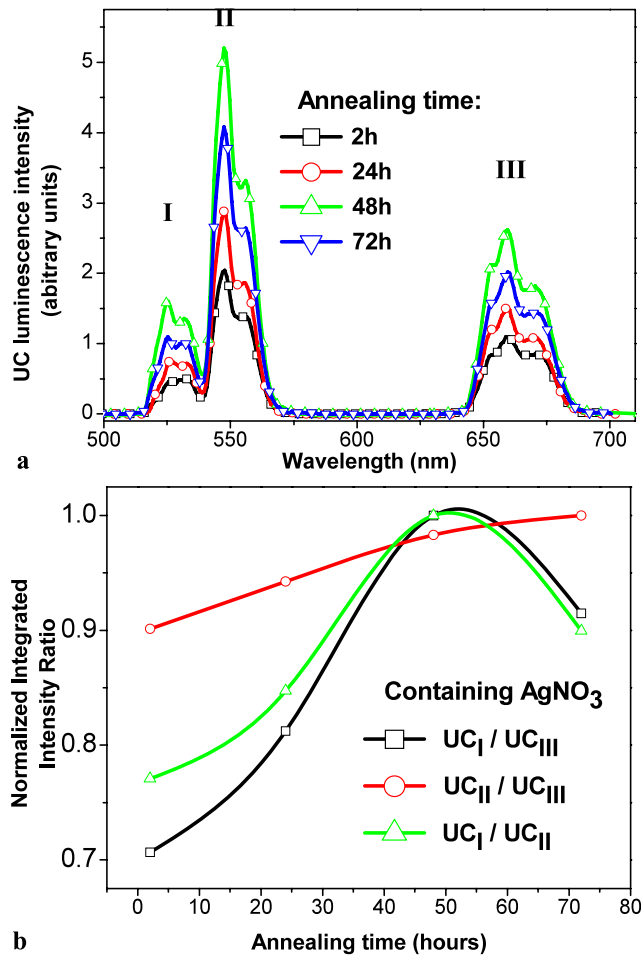
Fig. 4 Energy level diagram of Er^{3+} and Yb^{3+} ions illustrating possible UC pathways for the Er^{3+}–Yb^{3+}-codoped glasses. The *solid straight lines* with upward and downward arrows indicate optical transitions; *dotted lines* and *wavy arrows* denote ET processes and nonradiative relaxation, respectively

Fig. 3 (**a**) Frequency UC spectra for excitation at 980 nm. (**b**) Normalized integrated UC intensity as a function of the annealing time

because its oscillator strength is much greater than the one corresponding to the transition $^4I_{15/2} \to {}^4I_{11/2}$ (Er^{3+}), we attribute the excitation of levels $^4S_{3/2}$ and $^4F_{9/2}$ in Er^{3+} ions mainly to the ET from Yb^{3+} ions. The ET efficiency depends on the relative concentration of Er^{3+} and Yb^{3+} and the lifetime of the levels participating in the ET process.

There are two possible efficient ET pathways [12, 13] as indicated in Fig. 4 by the dashed lines 1, 2, and 3. The green emissions are mainly originated by the following process: Yb^{3+} ions are excited from the ground state to the $^2F_{5/2}$ multiplet under 980 nm pumping; the excited ions transfer the stored energy to the Er^{3+} ions that are promoted from the ground state to the $^4I_{11/2}$ state. Then, a second ET event promotes the Er^{3+} ions from the $^4I_{11/2}$ level to the $^4F_{7/2}$ level (steps (1) and (2)—dashed lines in the Fig. 4). Following this transition, the Er^{3+} ion relaxes nonradiatively to the $^2H_{11/2}$ and $^4S_{3/2}$ levels. Afterwards, the $^2H_{11/2} \to {}^4I_{15/2}$ and $^4S_{3/2} \to {}^4I_{15/2}$ transitions originate the green emissions. The proximity between the green luminescence wavelengths and λ_{SP} favors the intensity enhancement that is due to the
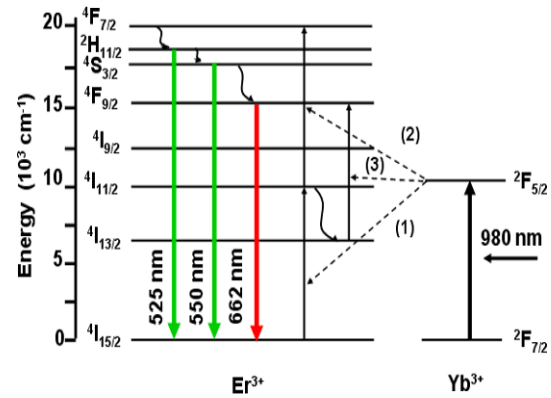
increased local field resulting from the mismatch between the dielectric functions of the silver NPs and the glass.

The red emission at 662 nm is due to the $^4F_{9/2} \to {}^4I_{15/2}$ transition. Besides the feeding of the $^4F_{9/2}$ level through the nonradiative relaxation from the $^4S_{3/2}$ level, the ET event represented by 3 in Fig. 4 may occur following the nonradiative transition $^4I_{11/2} \to {}^4I_{13/2}$. The longer lifetime of the $^4I_{13/2}$ level compared with the lifetime of the $^4I_{11/2}$ level [1] makes channel 3 dominant over channels 1 and 2; consequently, the red emission is enhanced. Moreover, as shown in Fig. 3, the red emission is also intensified for larger values of τ_A. This is attributed to the nucleation of larger silver NPs and aggregates as observed for Pr^{3+} in [7, 9]. Notice that the red intensity illustrated in Fig. 3 becomes comparable with the intensity of transitions $^2H_{11/2} \to {}^4I_{15/2}$ and $^4S_{3/2} \to {}^4I_{15/2}$ for $\tau_A \approx 40$ h. We also note from Fig. 3b that the ratio UC$_I$/UC$_{II}$ between the integrated intensities of transitions centered at 525 and 550 nm changes from 0.77 (for $\tau_A \approx 0$) to ∼1.0 (for $\tau_A \approx 50$ h). This behavior is understood considering that the transition at 525 nm is closest to λ_{SP} than 550 nm.

In summary, with the present results we demonstrated the simultaneous exploitation of the enhanced local field contribution due to silver NPs and energy transfer processes between two different rare-earth (RE) ions in order to control the luminescence spectrum of a glassy composite material. This approach can be applied for different RE ions in order to improve the efficiency of luminescent glasses.

References

1. M. Yamane, Y. Asahara, *Glasses for Photonics* (Cambridge University Press, Cambridge, 2000)
2. P.N. Prasad, *Nanophotonics* (Wiley, New York, 2004)
3. O.L. Malta, P.A.S. Cruz, G.F. de Sá, F. Auzel, J. Lumin. **33**, 261 (1985)
4. T. Hayakawa, S.T. Selvan, M. Nogami, Appl. Phys. Lett. **74**, 1513 (1999)
5. C. Strohhöfer, A. Polman, Appl. Phys. Lett. **81**, 1414 (2002)
6. J. Kalkman, L. Kuipers, A. Polman, Appl. Phys. Lett. **86**, 041113 (2005)
7. L.P. Naranjo, C.B. de Araújo, O.L. Malta, P.A.S. Cruz, L.R.P. Kassab, Appl. Phys. Lett. **87**, 241914 (2005)
8. R. de Almeida, D.M. da Silva, L.R.P. Kassab, C.B. de Araújo, Opt. Commun. **281**, 108 (2008)
9. V.K. Raí, L. de S. Menezes, C.B. de Araújo, L.R.P. Kassab, D.M. da Silva, R.A. Kobayashi, J. Appl. Phys. **103**, 093526 (2008)
10. D.M. da Silva, L.R.P. Kassab, S.R. Luthi, C.B. de Araújo, A.S.L. Gomes, M.J.V. Bell, Appl. Phys. Lett. **90**, 081913 (2007)
11. L.R.P. Kassab, C.B. de Araújo, R.A. Kobayashi, R. de A. Pinto, D.M. da Silva, J. Appl. Phys. **102**, 103515 (2007)
12. F.A. Bomfim, J.R. Martinelli, L.R.P. Kassab, N.U. Wetter, J.J. Neto, J. Non-Cryst. Solids (2008, to be published)
13. L. Feng, J. Wang, Q. Tang, H. Hu, H. Liang, Q. Su, J. Non-Cryst. Solids **352**, 2090 (2006)
14. E.D. Palik, *Handbook of Optical Constants of Solids* (Academic Press, New York, 1985)